Propagation Modeling Through Foliage in a Coniferous Forest at 28 GHz

Yaguang Zhang, Christopher R. Anderson, Nicolo Michelusi, David J. Love, Kenneth R. Baker, and James V. Krogmeier

Abstract—The goal of this article is to investigate the propagation behavior of 28-GHz millimeter wave in coniferous forests and model its basic transmission loss. Field measurements were conducted with a custom-designed sliding correlator sounder. Relevant foliage regions were extracted from high-resolution LiDAR data and satellite images. Our results show that traditional foliage analysis models for lower-frequency wireless communications fail to consistently output correct path loss predictions. Novel site-specific models are proposed to resolve this issue, yielding a 0.9 dB overall improvement and as much as a 20 dB regional improvement in root mean square errors.

Index Terms—Channel modeling, coniferous forest environments, millimeter wave, site-specific models.

I. Introduction

ITH the rapid standardization process of 5G communication networks [1], millimeter waves (mmwaves) have garnered great attention worldwide from industry, academia, and government. A major issue here is better understanding the propagation characteristics of mm-wave signals. Many mm-wave channel measurement campaigns have recently been carried out for urban and suburban environments [2]-[5]. However, very limited effort has been put into validating and improving currently available channel models in overcoming vegetation blockages. In [6], a constant excess path loss of around 25 dB was observed at 28.8 GHz through a pecan orchard for paths with roughly 8 to 20 trees. More recent works [5], [7] reported low attenuation values per unit foliage depth of 0.07 dB/m at 28 GHz and of 0.4 dB/m with 3 dB deviation at 73 GHz, respectively. Moreover, even though a variety of modeling approaches have been considered, most of them ignore site-specific geographic features [5]. A comprehensive analysis for attenuation in vegetation is required to validate those observations, showcase different modeling approaches, and make improvements to mm-wave propagation modeling.

We explore this research gap by investigating the mm-wave propagation at 28 GHz through vegetation. Using a portable custom-designed sliding correlator sounder, we carried out a measurement campaign in a coniferous forest near Boulder, Colorado and obtained a total of 1415 basic transmission loss measurements. Relevant foliage regions were extracted from

Y. Zhang, N. Michelusi, D. J. Love, and J. V. Krogmeier are with the School of Electrical and Computer Engineering, Purdue University, 465 Northwestern Avenue, West Lafayette, IN 47907, USA (Email: {ygzhang, michelus, djlove, jvk}@purdue.edu).

C. R. Anderson is with the Department of Electrical and Computer Engineering, United States Naval Academy, 105 Maryland Ave, Annapolis, MD 21402, USA (Email: canderso@usna.edu).

K. R. Baker is with the Interdisciplinary Telecommunications Program, University of Colorado Boulder, UCB 530, Boulder, CO 80309, USA (Email: ken.baker@colorado.edu).

Sponsorship for this work was provided by NSF research grant 1642982.

the United States Geological Survey (USGS) LiDAR and terrain elevation data. Tree locations were also manually labeled according to the LiDAR data and to high-resolution satellite images from Google Maps. These data enabled us to view channel modeling in a site-specific manner. A comprehensive model comparison is provided to elucidate the pros and cons of different modeling approaches for predicting signal attenuation through vegetation. Novel site-specific models with consistently better performance than existing models are developed. They are fully automatic, easy to implement, and feasibly applicable to machine learning frameworks.

II. MEASUREMENT SETUP

The measurement system in our previous work [4] was utilized. The receiver (RX), which had a chip rate of 399.95 megachips per second, was installed in a backpack and powered by a lithium-ion polymer battery for portability purposes. As illustrated in Fig. 1(a), the transmitter (TX) was set up at the edge of the forest, while the RX was moved in the coniferous forest to continuously record the signal along with the GPS-based location information. Basic transmission losses were computed accordingly. The TX antenna was adjusted before each signal recording activity to point to the middle area of the track to be covered. Beam alignment was achieved at the RX side using a compass. The site-specific geographic features of the forest are illustrated in Fig. 1(b).

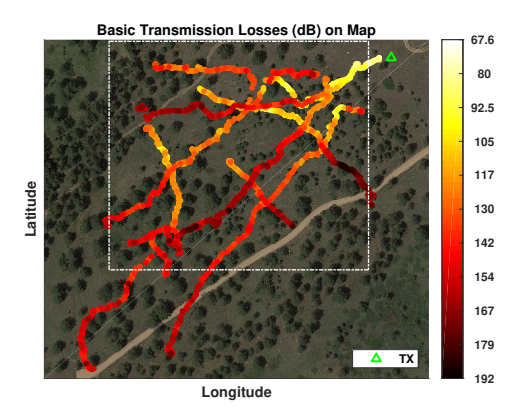
III. FOLIAGE ANALYSIS FOR THE CONIFEROUS FOREST

We compared three empirical foliage analysis models: the partition-dependent attenuation factor (AF) model [8], the ITU-R obstruction by woodland model [9], and Weissberger's model [10]. To tune these models, four parameters were computed for each measurement location: the distance between the TX and the RX, the number of tree trunks within the first Fresnel zone, the foliage depth along the line-of-sight (LoS) path, and the foliage area within the first Fresnel zone. These computations were performed in a three-dimensional (3D) reference system using Universal Transverse Mercator coordinates (x, y) and altitude. Based on the results, site-specific models were introduced to improve path loss predictions.

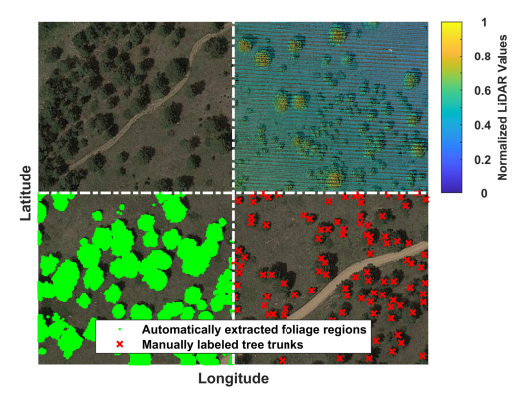
All channel models considered in the current paper generate excess attenuation values on top of a site-general channel model. Throughout our work, we use the free-space path loss (FSPL) model as the baseline generic model, that is, the path loss PL in dB at the RX location s is composed of two parts:

$$PL(s) = FSPL[d(s)] + EPL(s),$$

where FSPL[d(s)] is the FSPL in dB at a RX-to-TX distance of d at s, and EPL(s) is the excess path loss in dB at s.



(a) RX tracks illustrated with basic transmission loss results



(b) Site-specific information available for the measurement site

Fig. 1. Overview of the measurement campaign. (a) The TX was installed at the edge of a coniferous forest. The RX followed 10 different tracks. One basic transmission loss result was computed for each second of the recorded signal to match the GPS data. (b) We have zoomed in on the dotted-square area in (a) to better illustrate the site-specific features. Satellite images from Google Maps are used here as background. Overlaid on top are LiDAR data, foliage regions, and trunk locations, respectively.

A. The AF Propagation Model

The partition-dependent AF propagation model takes advantage of site-specific information by assuming each instance of one type of obstacle along the LoS path will incur a constant excess path loss. In our case, we counted the number of trees, N(s), along the LoS path to s and added a constant excess path loss in dB, L_0 , for each of the trees, as follows:

$$EPL(s) = N(s) \cdot L_0$$
.

There are different methods for determining N(s). Considering the forest size and the number of RX locations involved, it is extremely difficult and time-consuming to count N at each s on-site. In our work, we simplified the trees, making them vertical lines rather than estimating the cylinder of each tree. Then, the number of trees within the first Fresnel zone was estimated automatically in the 3D reference system for each s and used as the number of obstacle trees.

Fig. 2 shows the predictions obtained from the AF model. The unknown constant L_0 was fitted according to the measurement data, resulting in a value of 6.47 dB per tree. As can be seen, the AF model closely follows the shape formed by the measurement results. However, it suffers severely in foreseeing the correct amount of excess path loss in general. This is expected because we have only considered the trunk

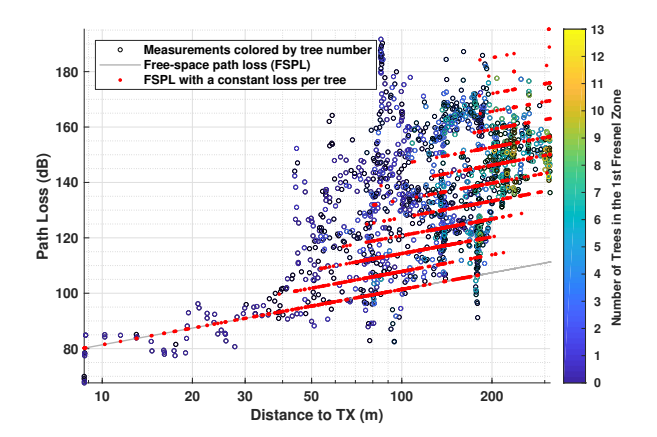


Fig. 2. The AF propagation model degenerates to a constant-loss-per-tree model in our case. Its predictions fit the shape of the measurement results but have a poor overall accuracy.

locations for counting trees, but the leaves and branches also play a critical role in attenuating the signal. The root mean squared error (RMSE) for the AF model compared with the measurements is 27.96 dB, achieving a 11.47 dB improvement over the FSPL model but still significantly worse than those for the other two empirical models discussed below.

B. ITU-R Obstruction by Woodland Model

The ITU-R obstruction by woodland model assumes one terminal (the TX or the RX) is located within woodland or similar extensive vegetation, which perfectly fits our measurement scenario. Instead of the number of trees, the ITU model uses the length of the path within the woodland in meters, $d_w(s)$, to estimate the excess path loss:

$$EPL(s) = A_m \left[1 - \exp(-d_w(s) \cdot \gamma / A_m) \right], \tag{1}$$

where $\gamma \approx 6$ dB/m is the typical specific attenuation for very short vegetative paths at 28 GHz, and A_m is the maximum attenuation in dB. The most distinguishing feature of this model is the upper limit imposed on the excess path loss.

Since the TX was installed approximately 15 m away from the forest, this offset has been taken away from the 3D RX-to-TX distance to estimate $d_w(s)$, with the negative results clipped to zero. Also, A_m is yet to be determined in [9] for 28-GHz signals, so we fitted it to our measurement results to obtain the best possible performance, which yielded $A_m \approx 34.5$ dB. The resulting predictions are plotted in Fig. 3. The ITU model excels in following the trend of the measurements, with an overall RMSE of 20.08 dB, the best among the empirical models considered. However, this model clearly overestimates the path loss for locations with d_w smaller than 30 m. At those locations, the LoS path may be clear or blocked by only a couple of trees, differing from a typical woodland blockage scenario. On the other hand, the ITU model underestimates the path loss for large d_w .

C. Weissberger's Model

Weissberger's model, or Weissberger's modified exponential decay (WMED) model, can be formulated as follows:

$$EPL(s) = \begin{cases} 0.45 \ f^{0.284} \ d_f(s) & \text{, if } 0 < d_f(s) \le 14 \\ 1.33 \ f^{0.284} \ d_f^{0.588}(s) & \text{, if } 14 < d_f(s) \le 400 \end{cases}$$

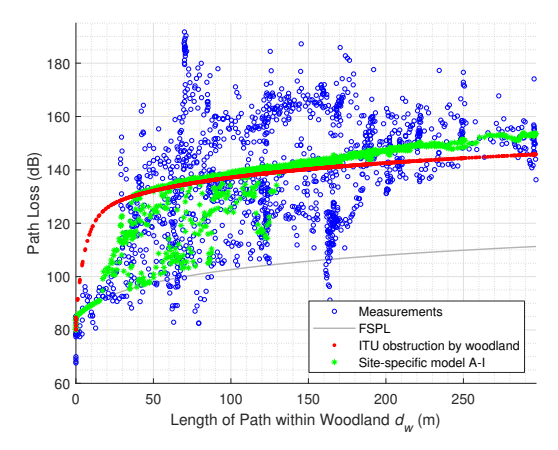


Fig. 3. Predictions from the ITU obstruction by woodland model. As a comparison, the predictions from one site-specific model, which is covered in Section III-D, are also shown. The site-specific model follows the measurements better than the ITU model at the lower and higher ends of d_w .

where f is the carrier frequency, and $d_f(s)$ is the foliage depth in meters along the LoS path for the RX location s. The model treats locations with deep-enough foliage, that is, $d_f(s) > 14$, differently from those with less foliage blockage.

Fig. 4(a) compares the predictions from the WMED model with the measurement results. Foliage depths have been computed via the site-specific geographic information, which gives a reasonably good RMSE value of 22.19 dB.

We have taken an image processing approach to obtain site-specific foliage depths, $d_f(s)$. Both the LiDAR data and the terrain elevation data from the USGS were rasterized onto the same set of reference location points. The foliage regions were then extracted by thresholding their difference, resulting in the foliage regions illustrated in Fig. 1(b). Along the LoS path, the ratio of the number of foliage region pixels over the total number of pixels was calculated and multiplied with the corresponding 3D RX-to-TX distance to get the foliage depth for each RX location s.

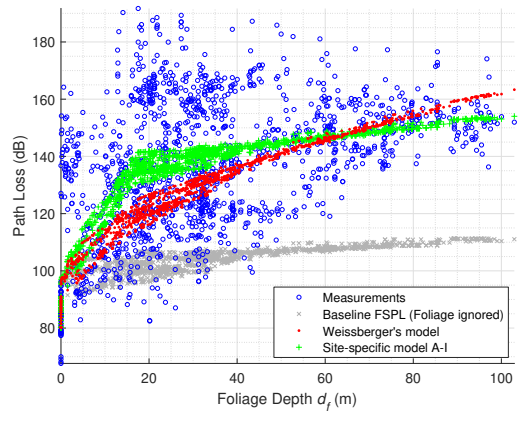
D. Site-specific Models

With high-precision geographic information that is available publicly for terrain modeling, such as the LiDAR data, existing channel models can be tuned accordingly with well-estimated site-specific parameters. Beyond that, some simple but powerful site-specific models can be constructed as alternatives. We refer to these as "site-specific" models because their performance depends heavily on the accuracy of the parameters evaluated for each site, for example, the 3D LoS distance and the foliage depth.

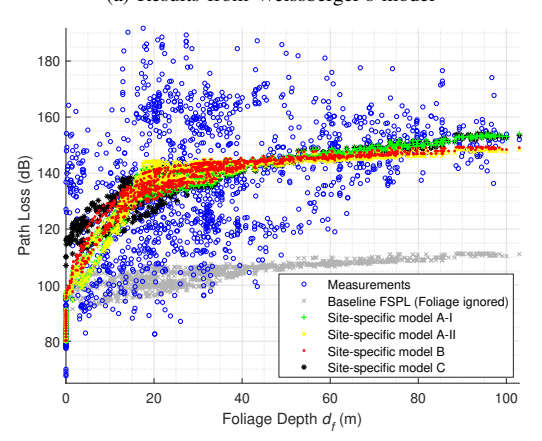
By combining the idea of considering obstacles individually for each *s* from the AF model and the two-slope modeling approach in the WMED model, we constructed *model A-I*:

$$EPL(s) = \begin{cases} d_f(s) \cdot L_1 \ , & \text{if } 0 \leq d_f(s) \leq D_f \\ D_f L_1 + \left[d_f(s) - D_f \right] L_2 \ , & \text{if } d_f(s) > D_f \end{cases}$$

where $d_f(s)$ is the foliage depth in meters at s, L_1 and L_2 are two constants for adjusting the extra loss in dB caused by each meter of foliage, and D_f is the boundary determining when



(a) Results from Weissberger's model



(b) Results from site-specific models

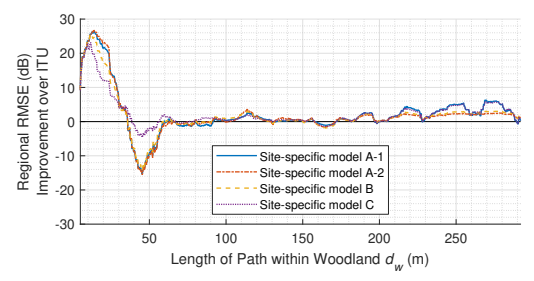
Fig. 4. Predictions from foliage-depth-based models. The baseline FSPL values, which have been evaluated individually for all RX locations without considering the foliage, are also shown for reference. They form a cloud because the foliage depth, d_F , does not increase linearly with the RX-to-TX distance. (a) Weissberger's model slightly underestimates the loss of RX locations with shallow vegetation blockages and overestimates the loss of those with deep vegetation blockages. To better illustrate this, results from *site-specific model A-I* are shown as a reference. (b) The site-specific models have very competitive performance. Results from *model C*, which makes predictions based on the foliage area in the first Fresnel zone, are also plotted here.

 L_2 will take effect. The upper bound from the ITU model can be imposed by setting $L_2 = 0$ to form *model A-II*:

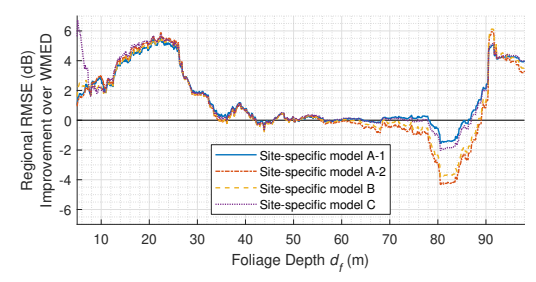
$$EPL(s) = \begin{cases} d_f(s) \cdot L_1 \text{, if } 0 \le d_f(s) \le D_f \\ D_f \cdot L_1 \text{, if } d_f(s) > D_f \end{cases}$$

We also reused the ITU model in Equation (1) with site-specific foliage depth to form *model B*. That is, $d_f(s)$ is used instead of $d_w(s)$, and parameters A_m and γ are set according to the measurements.

For a fair performance comparison for these three models, we used the WMED boundary $D_f=14$ for model A-I to leave only two parameters that are adjustable. After fitting these models to our data, we found $L_1\approx 2.39$ dB/m and $L_2\approx 0.12$ dB/m for model A-I, $L_1\approx 2.09$ dB/m and $D_f\approx 17.87$ m for model A-II, along with $A_m\approx 38.04$ dB and $\gamma\approx 4.47$ dB/m for model B. The resulting predictions are plotted in Fig. 4(b). The corresponding RMSE values are summarized in Table I, together with those for the traditional models as references. Note that the site-specific models perform very similarly, and each unit of foliage depth tends to contribute less to the excess



(a) Regional RMSE improvement over the ITU model



(b) Regional RMSE improvement over the WMED model

Fig. 5. Regional performance improvement for site-specific models. A windows size of 10 m is used. (a) Compared with the ITU model, site-specific models work significantly better for locations close to the TX and reasonably better for those far away. However, models A-I, A-II, and B suffer a severe performance decrease for $d_w \in [35, 60]$ m, which is less of an issue for model C. (b) Compared with the WMED model, site-specific models again work reasonably better for extreme cases. A performance deterioration is observed at a foliage depth of around 80 m, where models A-I and C are less influenced.

TABLE I OVERALL PERFORMANCE

	Baseline	Traditional			Site-Specific			
Model	FSPL	AF	ITU	WMED	A-I	A-II	В	С
RMSE (dB)	39.43	27.96	20.08	22.19	19.96	20.02	19.93	19.18

loss as foliage depth grows. *Model A-I* does not limit the excess loss as the other two site-specific models do, but it performs slightly better than *model A-II* in terms of the RMSE. Overall, *model B* performs the best, but computationally, it is more demanding because of its exponential form.

We can further push the best RMSE performance to 19.18 dB with *Model C*:

$$EPL(s) = \begin{cases} 0 \ , & \text{if } a_f(s) = 0 \\ a_f(s) \cdot L_1 + L_0 \ , & \text{if } 0 < a_f(s) \leq A_f \\ A_f L_1 + \left[a_f(s) - A_f \right] L_2 \ , & \text{if } a_f(s) > A_f \end{cases}$$

where $a_f(s)$ is the foliage area in square meters in the first Fresnel zone at RX location s; L_0 (dB), L_1 (dB/m²), and L_2 (dB/m²) are constants adjusting the excess loss contribution; and A_f is the boundary determining when the foliage is deep enough for L_2 to take effect. According to our measurement results, we have $L_0 \approx 19.14$ dB, $L_1 \approx 2.09$ dB/m², $L_2 \approx 0.06$ dB/m², and $A_f \approx 18.02$ m². The prediction results are also shown in Fig. 4(b) for reference.

The most important feature for these site-specific models is their consistently good performance throughout the whole dataset. To demonstrate this, regional RMSE improvements over the ITU and WMED models are evaluated in terms of d_w and d_f , respectively, as summarized in Fig. 5. For our data set, the ITU model works very well, as shown in Table I. However, according to Fig. 5(a), the ITU model suffers from an RMSE

degradation by as much as 20 dB compared with site-specific models in the low-vegetation-coverage region (d_w <30 m). An RMSE improvement of as much as 6 dB can be observed for large d_w values. A visual comparison for predictions from the ITU model and *site-specific model A-I* is provided in Fig. 3, where *model A-I* clearly works better for extreme cases at the low and high ends of d_w . Similar comparisons have been carried out for the WMED model in Fig. 5(b) and Fig. 4(a). The WMED model slightly underestimates the path loss at RX locations with a small d_f and overestimates the path loss at those with a large d_f . It is worth noting that empirical models do work significantly better in some distance regions, whereas *model C* normally suffers less in those regions.

IV. CONCLUSION

A comprehensive channel model comparison for attenuation through vegetation was conducted using data from measurements in a coniferous forest near Boulder, Colorado. The partition-dependent AF model is intuitive and site-specific but hard to automate with satisfying performance. The ITU obstruction by woodland model works extremely well overall, but only for scenarios with a moderate amount of foliage blockage. Weissberger's model is similar. By merging the existing models, site-specific models are proposed for consistent performance through shallow to deep vegetation blockages. These models are easy to implement and adaptable to machine-learning frameworks.

REFERENCES

- S. A. Busari, S. Mumtaz, S. Al-Rubaye, and J. Rodriguez, "5G millimeter-wave mobile broadband: Performance and challenges," *IEEE Communications Magazine*, vol. 56, no. 6, pp. 137–143, June 2018.
- [2] T. S. Rappaport, S. Sun, R. Mayzus, H. Zhao, Y. Azar, K. Wang, G. N. Wong, J. K. Schulz, M. Samimi, and F. Gutierrez Jr., "Millimeter wave mobile communications for 5g cellular: It will work!" *IEEE Access*, vol. 1, no. 1, pp. 335–349, 2013.
- [3] T. S. Rappaport, G. R. MacCartney, S. Sun, H. Yan, and S. Deng, "Small-scale, local area, and transitional millimeter wave propagation for 5G communications," *IEEE Transactions on Antennas and Propagation*, vol. 65, no. 12, pp. 6474–6490, 2017.
- [4] Y. Zhang, D. J. Love, N. Michelusi, J. V. Krogmeier, C. R. Anderson, S. Jyoti, and A. Sprintson, "28-GHz channel measurements and modeling for suburban environments," in 2018 IEEE International Conference on Communications (ICC). IEEE, May 2018, pp. 1–6.
- [5] Y. Zhang, D. J. Love, N. Michelusi, J. V. Krogmeier, S. Jyoti, A. Sprintson, and C. R. Anderson, "Improving millimeter-wave channel models for suburban environments with site-specific geometric features," in 2018 International Applied Computational Electromagnetics Society (ACES) Symposium. IEEE, 2018, pp. 1–2.
- [6] P. B. Papazian, D. L. Jones, and R. H. Espeland, "Wideband propagation measurements at 30.3 GHz through a pecan orchard in texas," National Telecommunications and Information Administration (NTIA), Boulder, CO, Tech. Rep. 92-287, September 1992.
- [7] T. S. Rappaport and S. Deng, "73 GHz wideband millimeter-wave foliage and ground reflection measurements and models," in 2015 IEEE International Conference on Communication Workshop (ICCW). IEEE, 2015, pp. 1238–1243.
- [8] G. Durgin, T. S. Rappaport, and H. Xu, "Measurements and models for radio path loss and penetration loss in and around homes and trees at 5.85 GHz," *IEEE Transactions on Communications*, vol. 46, no. 11, pp. 1484–1496, 1998.
- [9] International Telecommunication Union, Recommendation ITU-R P.833-9 Attenuation in vegetation, Std., September 2016. [Online]. Available: https://www.itu.int/rec/R-REC-P.833-9-201609-I/en
- [10] M. A. Weissberger, "An initial critical summary of models for predicting the attenuation of radio waves by trees," Electromagnetic Compatibility Analysis Center, Annapolis, MD, Tech. Rep. ESD-TR-81-101, 1982.